

Computational Investigation of Thermal Performance of Solar Air Heater Having Roughness Elements as a Bend on the Absorber Plate

Suman Kumar Saurabh¹, Ashutosh Kumar^{2*}

Submitted: 02/04/2023

Revised: 12/07/2023

Accepted: 11/08/2023

Abstract: An Analytical investigation has been carried out to study the heat transfer and friction characteristics by using a bend roughness on the absorber plate of a solar air heater. The Analytical investigation consist the Reynolds number (Re) ranges from 18000 to 50000, relative roughness pitch (p/h) is 0.5-3 and relative roughness (p/D_b) 4.29-12. The effect of these parameters on the heat transfer coefficient and friction factor has been discussed in the present report and correlations for Nusselt number and friction factor has been developed within above limits. A procedure to compute the thermal efficiency based on heat transfer processes in the system is also given and the effect of these parameters on thermal efficiency has been discussed. Bend as roughness elements have been used to enhance heat transfer coefficient. By providing artificial roughness it has been concluded that there is an improvement of heat transfer and temperature enhancement.

Keyword – solar energy, heat transfer, relative roughness pitch, thermal efficiency

1.1 Introduction

Energy is most fundamentally the ability to do work. All of the achievements of mankind were sustained through the use of energy. At the root of modern society is the ability to harness energy. Energy has always been among the most fundamental elements for the survival, reproduction and evolution of human society. The modern world runs on energy. This might seem obvious, but in terms of history, it is rather a dramatic development. Prior to the industrial revolution, human society used very little energy beyond what human labour, animal power, and what basic natural resources like wind, water and fire could provide. But once the industrial revolution hit, suddenly it became necessary to find new sources of energy to power a world increasingly run by machine. Over the course of the last two centuries, we have gone from a world

powered by wood, whale blubber, wind, and river water to one in which fossil fuels, solar panels, and even nuclear fission help to feed humanity's ever-growing need for more and more energy. As the rate of energy consumption continues to grow, competition for dwindling energy resources only makes it more difficult and expensive to keep up the same levels of consumption. One of the reasons that energy resources are so important is that they make it possible for a country to maintain its lifestyle. When China became a world power and announced its plan to develop its standard of living through industrialization, securing energy resources became a matter of extreme concern. It was on the back of vast strip mining of fossil fuels that China developed its industrial base. A lack of natural resources can make it harder for a country to reach the highest levels of industrial development because it is usually more expensive to import fuel than it is to produce it at home. In present's world the prosperity of nation is measured by the energy consumption of that nation, the GDP of country is directly linked with energy consumption. Therefore demand for energy resources is increasing day by day. But the importance of

^{1,2}National institute of technology, Jamshedpur 831014

¹ORCID ID: <https://orcid.org/0000-0003-4085-3211>

*Corresponding Authors_ashu101634@gmail.com

energy resources isn't just found at the international level. Right in our own home, we have to make decisions about which energy resources to use to heat, cool, and power your home. Most homes are heated either through oil, natural gas, or electricity. Some even use wood-burning stoves. Each of these has pluses and minuses, and each utilizes a different energy resource system in order to create heat. Fortunately, we live in an age when it is possible to make use of a wider variety of energy resources. The choice of which resource to use impacts not just individuals

but also the environment. Some resources are renewable, some are not, and some, such as nuclear, run the risk of damaging the environment for generations to come. Whatever energy choice we make, there are consequences to consider. The good news is that in today's world there have never been so many options for making responsible choices that will benefit the environment, or at least reduce the risks so that the future will have plenty of energy resources for everyone. A brief Classification of energy resources is represented in Fig 1.1

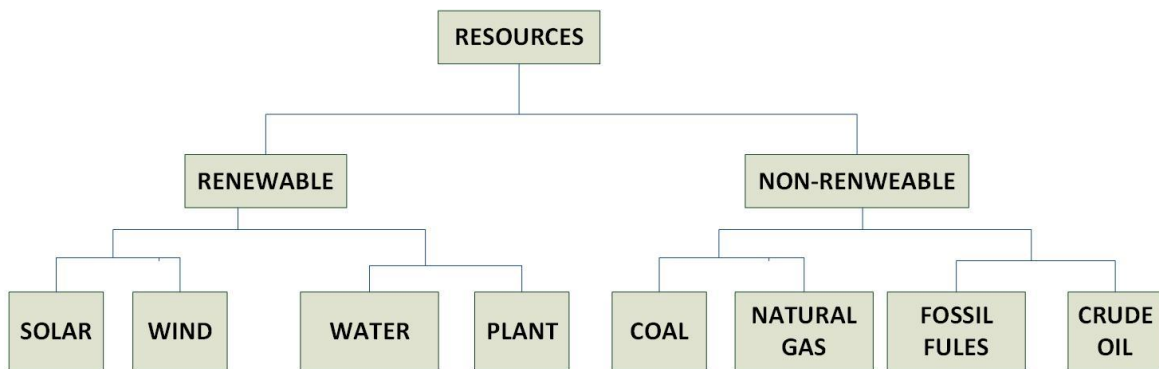


Fig 1.1 Classifications of Energy Resources

Spectrum of solar radiation extends from 200 to 3000 nm in wavelength. It is almost identical with the 6000 K black body radiation spectrum. The radiation is distinguished as:

The principle behind a flat plate collector is simple. If a metal sheet is exposed to the solar radiation, the temperature will rise until the rate at which energy is received is equal to the rate at which heat is lost from the plate; this temperature is termed as 'equilibrium temperature'. If the back and side of the plate are protected by a heat insulating material, and the exposed surface of the plate is painted black and is covered by one or two glass sheets, then the equilibrium temperature will be much higher than that for the simple exposed sheet. The plate may be converted into an air heater or water heater by passing air/water through the plate by ensuring sufficient heat transfer arrangement.

1.2 Solar Air Heater

Compared to other solar collectors, solar air heaters (SAH) have some distinct advantages. The mode of heat transfer from the absorber plate and the working fluid is the main difference between liquid

flat plate collectors and air heaters. The air heaters eliminate the need to transfer heat from the working fluid to another working fluid. Air is being directly used as the working substance, the system is less complicated and is compact. The corrosion problem, which can become serious in solar water heater, is completely eliminated in solar air heaters. Hence light gauge steel or aluminium plates can easily be used. Hence, a solar air heater appears to be inherently cheaper and can last longer. Unlike liquid flat plate collectors, system is not pressurized and therefore, light gauge metal sheets can be used. In solar air heaters leakage is also not a big problem, unlike in liquid collectors. One of the major problems in improperly designed air heating collectors is the poor heat transfer from the absorber plate to the air. The heat transfer coefficients can be considerably improved in several ways, and efficiencies comparable to those of liquid flat plate collectors can be obtained by properly designing the air heater. Owing to the low density of air, large volume of air has to be handled, in comparison with the volume of liquid required to collect the same amount of heat.

Another disadvantage is the low thermal capacity of air. The principle of solar air heater is virtually the same as that of the liquid flat plate collector. Air is circulated in contact with a black radiation-absorbing surface, which is usually overlaid by one or more transparent covers for heat loss reduction. Solar air heaters are of many types. In some of these, the absorber surface beneath the glazing includes overlapped, spaced, clear and black glass plates, single smooth metal sheets.

1.2 Literature survey

The thermal performance of conventional solar air heaters has been found to be poor because of the low convective heat transfer coefficient from the absorber plate to the air. Convective heat transfer is low between air and absorber plate due to formation of laminar sub-layer which acts as thermal barrier between air and absorber plate.

So there is a need to break the laminar sub layer therefore, artificial roughness has been used extensively for the enhancement of forced convective heat transfer, which further requires flow at the heat-transferring surface to be turbulent. However, energy for creating such turbulence has to come from the fan or blower and the excessive power is required to flow air through the duct. Therefore, it is desirable that the turbulence must be created only in the region very close to the heat transferring surface, so that the power requirement may be reduced. Amraoui et al [1]. Flat plate solar collectors are the most common thermal collectors used among the various solar collectors for domestic and industrial purposes. The objective of this study is to perform computational fluid dynamics (CFD) simulation of flat plate collector with air flow. In this paper, the CFD tool has been used to simulate the solar collector for better understanding of its heat transfer capability. Using a 3D model of the collector involving air inlet, the collector is modeled by ANSYS Workbench and the grid was created in ANSYS ICEM. The results were obtained by using ANSYS FLUENT. The objective of this work is to compare theoretical and experimental achieved work toward the given work by using CFD tool with respect to flow and temperature distribution inside the solar collector. The outlet temperature of air was compared with experimental results and there was a good agreement between them.

Singh et al [2]. thermo-hydraulic performance was analyzed computationally for the stationary

channels with rib turbulators situated at right angles i.e. 90 degrees and then optimized by employing Taguchi approach. Ribs were arranged in a linear manner one after another and numerical values of the friction factor and convective heat transfer coefficient were computed. AL16 (43) orthogonal array has been taken for optimization purpose for maximization of thermal performance. The concept of thermal performance includes the twofold effects at a same time i.e. it maximizes the heat transfer coefficient and at the same time minimizes the friction factor. Maximization of thermal enhancement factor is considered as the ultimate aim of present work. The rib relative pitch (p/e) is varied as 3, 6, 9 and 12. The inclination angles are varied from 45° to 90° in a step of 15 degree thereby leading different rib shapes i.e. right angled triangle, trapezoidal and square ribs. Different values of heat transfer coefficient and friction factors were computed by varying Reynolds numbers 4000, 8000, 12,000, 16,000. By combined effect of rib pitch-to-height ratio, inclination angles and flow parameters, the optimal cooling configuration was obtained. A right triangular shaped rib with optimum parameters (α) = 45° , $Re = 4000$, and $p/e = 9$ has found best for thermo-hydraulic performance against square rib. Mukesh K. [3] experimental study has been done on a low porosity packed bed solar air heater. Investigation covers a widerange of geometrical parameters of wire screen matrices, i.e. wire diameter 0.48 mm, pitch 2.3 mm and number of layers from 3-6 and low range of porosity from 0.9614-0.9807 and packing Reynolds number range from 1064-2405. It is seen that heat transfer coefficient and friction factor are strong functions of geometrical parameters of the porous packed bed. A decrease in porosity increases the volumetric heat transfer coefficient.

Kardi et al [4]. The solar energy for thermal applications has emerged as a focus research area in the light of growing concern about environmental degradation on account of fossil fuel usage. The worldwide impetus to go green strategy has imposed a peculiar and important constraint to engineering solutions to imbibe sustainability concepts. The current research is focussed to promote renewable energy in all possible domains so as to mitigate green house emissions. The huge potential of solar energy is at human disposal, but not coherent with our designs that need innovations to match the potential with energy conversion

devices. The role of Computational Fluid Dynamics(CFD) that has emerged as a popular modeling approach based on numerical methods and computer simulations to solve and analyze problems involving complex fluid flow has become important. CFD-based models demonstrate high versatility and capability of dealing with a wide range of engineering problems. This article presents CFD-based modeling of solar flat plate air heater with chamfered fin geometry with respect to configuration at collector inlet. The influence of a number of inlet openings, mass flow rate and incident solar insolation were simulated and discussed. The obtained results were verified through with experimental results that evidenced enhancement in heat transfer without penalty of frictional losses.

Priyam et al 5].The thermal performance of a solar air heater with wavy fins attached were investigated theoretically. The fluid channel has been formed by using wavy fins parallel to fluid flow below the absorber plate. The effects of mass flow rate and fin spacing on the thermal performance and rise in temperature were studied. The indicated results show that fin spacing of 1 cm yields maximum thermal efficiency and the maximum enhancement of 1.29 times in thermal efficiency has been obtained with the use of wavy fins as compared to longitudinal fins. Also, a maximum enhancement in temperature rise has been found as 1.25 times as compared to longitudinal fins at lower mass flow rate of 0.0134kg/s. Anil Kumar[6].An artificial roughness on the heat transfer surface in the form of projections mainly creates turbulence near the wall or breaks the laminar sub-layer and thus enhances the heat transfer coefficient. In the present work the performance of a solar air heater duct provided with artificial roughness in the form of thin circular wire in V-shaped, Multi v-shaped ribs and Multi v-shaped ribs with gap geometries has been analyzed using CFD. The effect of these geometries on heat transfer and friction factor and performance enhancement was investigated covering the range of roughness parameters V-shaped, Multi v-shaped ribs, Multi v-shaped ribs with gap and working parameters. Different turbulent models have been used for the analysis heat transfer and friction factor and their results are compared with Dittus-Boelter Empirical relationship for smooth surface. Renormalization k-epsilon model based results have been found in good agreement and

accordingly this model is used to predict heat transfer and friction factor in the duct.

On the basis of literature survey the of the researchers, who have studies solar air heater, infer that the efficiency of these heaters is poor primarily due to the presence of laminar sub layer at the interface of air and absorber plate. The performance is evaluated by creating artificial roughness on the inner surface of absorber plates. Few researchers recommended longitudinal rectangular array of fins and optimal conditions have been derived. From various researchers' point of view after conducting number of experiments, it was stated that, the inefficiency of solar air heater is due to the presence of laminar sub-layer at the interface of air and absorber plate. The same result was experienced even for turbulent flow of air. Some researchers studied the effect of artificial roughness through computational fluid dynamics (CFD). Various parameters such as roughness, height, angle, Reynolds number and solar radiation are considered while performing CFD analysis. It was clearly understood that, the area of absorber plate, solar collector, pipe diameter, mass flow rate, inlet and outlet temperature of fluid show their impact on the performance of Solar system. Most of the researchers worked on various types of roughness elements for increasing the surface roughness of absorber plate by wire mesh, ribs, wires, dimples etc. They investigated the effect of roughness on only one side of the absorber plate.

In the present work, the problem is formulated by incorporating bend roughness on one side of the absorber plate. The effects of relative roughness pitch and relative roughness on the heat transfer rate and thermo hydraulic performance of the air heater are determined.

The correlations have been determined to find the combined effect of the Nusselt number and friction factor. Thermo-hydraulic performance which is an overall measure of heat transfer rate and friction factor has been evaluated. From the experimentation and results, it is aimed to determine the enhancement of heat transfer and the effect of relative roughness pitch and relative roughness of bend roughened on one side of absorber plate.

Hence, the present work is aimed at overcoming the effect of the laminar sub-layer formation by providing bend as roughness elements. There by the surface contact of the air with absorber plate

increases. This results in enhancement of heat transfer rate of the solar air heater

2.1 Methodology

In fully developed turbulent flow, theoretical approaches to the problem of heat transfer in smooth and rough tubes are being developed from many years. This theoretical approach offers a technique to carry out the investigation in an ordered way. Even though the approach may be based on fundamental concepts of convective heat transfer and fluid flow inside the rectangular ducts but it influences the design and investigation techniques and gives an approximate idea of the variation of the system performance based on the given input parameters.

These approaches are based on similarity considerations. The two surfaces are said to have geometrically similar roughness if the geometry of their roughness is the same in all aspects except for a scale factor. For example, sand grain roughness is a geometrically similar roughness. With repeated-rib roughness, for a given flow attack angle, rib shape and pitch to height ratio, tests with a different height to hydraulic diameter ratio represent geometrically similar roughness.

However, when the values of relative roughness pitch, relative roughness height, flow attack angle, relative roughness gap or rib cross sections are varied, the surfaces are not geometrically similar. Surfaces which are not geometrically similar will require modifications to the roughness and heat transfer functions found by similarity considerations.

At the outset, considering friction factors for geometrically similar roughness, the basic assumptions used are the velocity defect law and the law of the wall similarity. The first of these implies, for turbulent flow in a channel, the existence of a region, away from the immediate vicinity of the wall, where the direct effect of viscosity and roughness on the core flow is negligible. The second law of the wall similarity implies for turbulent flow channel i.e. at the existence of a region close to the wall where the velocity distribution depends on the local conditions such as the distance from the wall, density, kinematic viscosity, and shear stress and roughness height. Therefore in this study various parameters which disturbs velocity distribution in

laminar sub layer are considered for the theoretical analysis.

2.2 Characterization of turbulent duct flows

A turbulent boundary layer in a duct may be distinguished into four different regions. The very thin layer in the immediate vicinity of the duct wall where viscous effects are dominant is the viscous (or laminar) sub-layer. The velocity profile in this layer is very nearly linear, and the fluid particles move in an orderly streamlined pattern parallel to the duct wall. Next to the viscous sub-layer is the buffer layer, in which turbulent effects are becoming significant, but the flow is still dominated by viscous effects. Above the buffer layer is the overlap (or transition) layer, also called the inertial sub-layer, in which the turbulent effects are much more significant, but still not dominant. Above that is the outer (or turbulent) layer in the remaining part of the flow in which turbulent effects dominate over molecular diffusion (viscous) effects and chunks of fluid move in a totally chaotic pattern causing an intense mixing of the fluid.

The thickness of the viscous sub-layer is very small, but this thin layer next to the wall plays a dominant role on flow characteristics because of the large velocity gradients it involves. The wall dampens any eddy motion, and thus the flow in this layer is essentially laminar and the shear stress consists of laminar shear stress which is proportional to the fluid viscosity. Considering that velocity changes from zero to nearly the core region value across a layer, the profile in this layer to be very nearly linear.

Then the velocity gradient in the viscous sub-layer remains constant at

$$\frac{du}{dy} = \frac{u}{y}$$

And the wall shear stress can be expressed as follows.

$$\tau_w = \mu \frac{dy}{dx} = \rho \nu \frac{u}{y} \quad \text{or,} \quad \frac{\tau_w}{\rho} = \frac{uv}{y}$$

Where y is distance from wall.

$$\sqrt{\frac{\tau_w}{\rho}} = \text{friction velocity.}$$

$$\text{Rearranging,} \quad \frac{u}{\sqrt{\tau_w/\rho}} = \frac{y}{\nu} \sqrt{\tau_w/\rho} \quad \text{Or,} \quad u^+ = y^+$$

$$\text{Where } u^+ = \frac{u}{\sqrt{\tau_w/\rho}} \quad \text{and } y^+ = \frac{y}{\nu} \sqrt{\tau_w/\rho}$$

Above equation is known as law of wall and it is found to correlate experimental data for smooth surfaces for well for $0 \leq y^+ \leq 5$.

Therefore, the thickness of the viscous sub-layer is

$$y = \delta' = \frac{5\nu}{\sqrt{\tau_w/\rho}} = \frac{5\nu}{u}$$

Where, u is the flow velocity at the edge of the viscous sub-layer the above expression can also be expressed in terms of Reynolds number as:

$$\frac{\delta'}{D} = \frac{25}{Re}$$

δ' Represents the distance from the boundary at which the flow changes from being predominantly laminar to being predominantly turbulent. It is

important to know the Transition layer thickness (δ') because the roughness height should be comparable to (δ') to enhance heat transfer. The values of the parameter (δ'/D) define the limit of laminar sub-layer thickness. Also, the values of (δ'/D) helps to decide the roughness height required to break or interrupt the laminar sub-layer for a given hydraulic diameter (D) and Reynolds number.

2.3 Boundary wall

Law of the wall depicts dimensionless velocity u^+ as a function of dimensionless distance y^+ . The different zones of the velocity profile are represented as shown below **Table 2.1**

Table 2.1

| | | |
|----------------------------|-----------------------|----------------------|
| $u^+ = y^+$ | for laminar sub-layer | $0 \leq y^+ \leq 5$ |
| $u^+ = 5 \ln(y^+) + 3.5$ | for buffer layer | $5 \leq y^+ \leq 30$ |
| $u^+ = 2.5 \ln(y^+) + 5.5$ | for turbulent layer | $y^+ > 30$ |

The logarithmic velocity distribution of turbulent boundary layer is shown to extend up to $y^+ = 500$. For the range y^+ from 0 to approximately 500 the velocity distribution is called the law of the wall. Beyond $y^+ > 500$, velocity defect law applies.

The velocity defect law implies that the existence of a region away from the immediate vicinity of the wall, where the direct effects of viscosity and roughness on the core flow is negligible. The law of the wall implies for turbulent flow channel i.e. at the existence of a region close to the wall where the velocity distribution depends on the local conditions such as the distance from the wall, density, kinematic velocity, and shear stress and roughness height. Therefore in this study roughness height is used as one of the parameters to disturb the velocity distribution in laminar sub-layer.

2.4 Thermal performance

The rate of useful energy gain by the flowing air through the duct of a solar air heater is calculated by using the following equation

$$q = mC_p(t_o - t_i) = hA_c(t_p - t_a)$$

From the above equation it is evident that useful energy gain mainly depends on the heat transfer coefficient (h). It can be represented in non-

dimensional form using following relationship of the Nusselt number (Nu).

$$Nu = \frac{hD}{k}$$

Also, heat transfer coefficient (h) can be represented in non-dimensional form using following relationship of Stanton number (St)

$$St = \frac{Nu}{Re.Pr}$$

2.5 Hydraulic performance

Hydraulic performance of solar air heater concerns with pressure drop (Δp) in the duct. Pressure drops accounts for energy consumption by blower to propel air through ducts. Pressure drop can be represented in non-dimensional form by using following relationship of friction factor (f) exists

$$f = \frac{D \Delta p}{2LV^2\rho}$$

2.6 Solar Air Heater duct design

Fig. 3.1 represents the two side roughened solar air heater which is considered for the analysis. It has two side roughened wall and two side smooth wall, rough wall is shown in dark area. Absorber plate constitute of these two roughened wall. Its dimension is $W \times B$ shown in **Table 2.2**

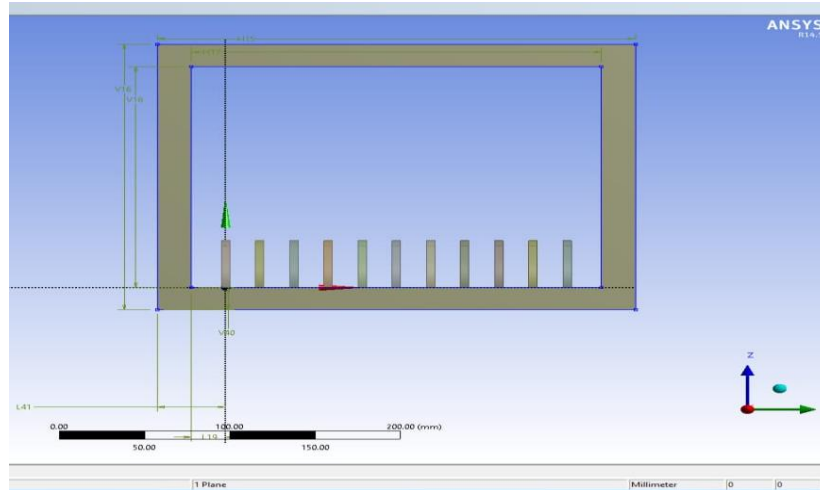


Fig 2.1 Flow passage of One side roughened solar collector duct.

Table 2.2 Dimensional parameter of collector and roughness

| Name | Symbol | Value |
|--------------------------------|----------|-------------------------------|
| Length of the duct | L | 1280 mm |
| Height of the duct | W | 150mm |
| Breadth of the duct | B | 240mm |
| Hydraulic diameter of the duct | D | 184.6mm |
| Bend Base Geometry | axa | 2.5mmx2.5mm; 5mmx5mm; 7mmx7mm |
| Angle of Arc of Bend | Ang. | 90 degree |
| Pitch | p | 30mm |
| Equivalence Diameter of Bend | D_b | 2.5; 5; 7 |
| Height of the roughness | h | 10-60 mm |
| Relative roughness pitch | P/h | 0.5; 0.6; 0.75; 1; 1.5; 3 |
| Relative Roughness | P/ D_b | 4.29; 6; 12 |

2.7 Theoretical analysis of bend roughened absorber solar air heater

Solar air heaters form the major component of solar energy utilization system. These solar air heaters generally have rectangular flow passage formed by two plates one of which is the absorber plate of the collector. This collector is the only surface, which absorbs the incoming solar radiation and converts it into thermal energy at the absorbing surface and transfers the energy to the flowing fluid through the collector.

In order to increase the heat transfer in solar air heater ducts artificial roughness is the form of transverse wire is found to be a convenient method. Small diameter wires are considered to be the roughness elements. Since, rounding of sharp corner shows a great reduction in friction factor. When compared to smaller roundness elements greater roundness element gives lower rates of heat transfer and lower friction. The range of parameters for this study is decided on the basis of practical considerations of the system and operating conditions. Roughness parameters selected include the height or diameter of the bend (e), the pitch of

the roughness element (p), Reynolds number (Re), relative roughness pitch and eight.

2.8 Fluid flow analysis

The purpose of analysing fluid flow is to determine the friction factor for two smooth sided and two rough sided duct for fully developed turbulent flow. Correlation for average friction factor is developed as a function of various geometrical parameters of artificial roughness used in the present investigation.

Friction factor for fully developed turbulent flow in a four side smooth duct, is given by the relation

$$f_s = \frac{\tau_s}{\frac{1}{2}\rho v_s^2}$$

Similarly, the friction factor for fully developed turbulent flow in a four-side rough duct, is given by the relation.

2.9 Heat transfer analysis

The prediction method for heat transfer will be very much similar to that of friction factor.

Assuming heat and momentum transfer analogy is valid.

Wall similarity law is used for temperature profile to correlate the heat transfer analysis with the assumption that the heat transfer roughness function, $GH(e^+, pr)$, is only depends on roughness geometry and it is independent of duct dimensions. According to Dalle Donne and Mayer, 1977 [20] the equation of Webb. Etal 1971 [21] can be used for similar roughness geometry which is given by

$$St_r = \frac{f_r/2}{1 + \sqrt{\left(\frac{f_r}{2}\right) \left[4.5(e^+)^{0.28} pr^{0.57} - 0.95\left(\frac{p}{e}\right)^{0.53}\right]}}$$

The values of average Nusselt number can be written as

$$\overline{Nu_r} = \overline{St_r} RePr$$

$$\overline{Nu_r} = \frac{\overline{f_r}/2}{1 + \sqrt{\left(\frac{\overline{f_r}}{2}\right) \left[4.5(e^+)^{0.28} pr^{0.57} - 0.95\left(\frac{p}{e}\right)^{0.53}\right]}} RePr$$

$$h = \frac{\overline{Nu_r} ka}{D}$$

2.10 Thermal performance analysis

Performance of a flat plate collector was first investigated by Hottel and Woertz (1942) [22]. It is assumed that the rate of useful heat collection is equal to the rate at which solar energy is being absorbed minus the heat loss rate. They proposed relationship for determining the rate of useful thermal energy collection of a flat plate collector, operating under quasi-steady state conditions as follows:

$$q_u = I(\tau\alpha) - U_L(t_p - t_a)$$

The term $(\tau\alpha)$ represents transmittance absorbance product, which accounts for the complex interaction of optical properties of the glass cover and absorber plate. In fact, the average absorber plate temperature depends upon geometry of collector, incident solar radiations, fluid flow rate and the properties of collector fluid. Bliss (1959) [23] proposed an alternative equation incorporating a new parameter F' , known as collector efficiency factor in terms of average fluid t_f temperature as follows:

$$q_u = F' [I(\tau\alpha) - U_L(t_f - t_a)]$$

Bliss (1959) [23] also modified Eq. (2.1) to a still more practically usable form as below:

$$q_u = F_R [I(\tau\alpha) - U_L(t_i - t_a)]$$

Where F_R is termed as collector heat removal factor. Hottel and Whillier (1955) [22]

obtained an expression for heat removal factor, as follows:

$$F_O = \frac{Gc_p}{U_L} \left[\exp \left(\frac{U_L F'}{Gc_p} \right) - 1 \right]$$

Solar collector efficiency η has been expressed as:

$$\eta = \frac{q_u}{I}$$

$$\eta = F_R \left[(\tau\alpha) - U_L \left(\frac{t_p - t_a}{I} \right) \right]$$

$$\eta = F' \left[(\tau\alpha) - U_L \left(\frac{t_f - t_a}{I} \right) \right]$$

$$\eta = F_R \left[(\tau\alpha) - U_L \left(\frac{t_a - t_a}{I} \right) \right]$$

These equations are widely used for comparing thermal performance of collectors and also to determine the effect of the changes in system and operating parameters on the collector efficiency.

Biondi *et al.* (1988) [24] have proposed following equations for efficiency of solar heater drawing ambient air:

$$\eta = F_o \left[(\tau\alpha) - U_L \left(\frac{t_o - t_i}{I} \right) \right]$$

Where F is the heat removal factor referred to outlet air temperature and is expressed as:

$$F_O = \frac{Gc_p}{U_L} \left[\exp \left(\frac{U_L F'}{Gc_p} \right) - 1 \right]$$

a) Overall Heat Loss Coefficient

An accurate determination of heat loss coefficient, U_L , is important for the determination of

solar collector efficiency. It is known that the overall loss coefficient is the sum of its component, namely: top, bottom and edge loss coefficients and U_e as written below:

$$U_L = U_t + U_b + U_e$$

Above relation can predict heat loss from top, bottom and edge side of the collector duct.

In our duct design heat in one edge side glass plate is present, since the height of the duct is very less as compared to the breath of the duct so the edge loss will also less as compared to the top loss coefficient. Therefore edge loss co-efficient is neglected in our performance investigation.

So, the overall heat loss co-efficient becomes:

$$U_L = U_t + U_b$$

b) Top loss coefficient

Tabor proposed top plate loss co-efficient can be calculated by:

$$U_T = \left[\frac{N}{\left(\frac{c}{t_p} \right)^{N+f} + \frac{1}{h_w}} \right]^{-1} + \frac{\sigma(t_p - t_a)(t_p^2 - t_a^2)}{\left[\varepsilon_p + 0.05N(1 - \varepsilon_p) \right]^{-1} + \left[\frac{2N + f - 1}{\varepsilon_g} \right]^{-1} - N}$$

$$f = (1 - 0.04h_w + 0.005h_w^2)(1 + 0.091N)$$

$$c = 365.9(1 - 0.00883\beta + 0.0001298\beta^2)$$

Here h_w is a convection coefficient and its value, as suggested by McAdams is

$$h_w = 5.7 + 3.8V_w$$

Here V_w is air flowing velocity.

c) Bottom loss coefficient

Considering the conductive heat transfer through insulation and convective heat transfer

From Bottom of the collector to environment, bottom loss coefficient is calculated as follows:

$$U_b = \left[\frac{t}{k_i} + \frac{1}{h_b} \right]^{-1}$$

Assuming the bottom side convective heat loss coefficient is very less so it can be neglected

without considerable effect on the performance.

Therefore bottom loss coefficient becomes

$$U_b = \frac{k_i}{t}$$

2.11 Thermal performance prediction

The thermal performance of solar air heater can be analysed based on the heat transfer process in the collector. By utilizing the correlation developed for heat transfer co-efficient.

(Nusselt number) and friction factor, various loss co-efficient and gain factors are calculated which is used for estimating the efficiency of the solar collector.

Data used performance prediction calculation

The following data has been utilized for the efficiency prediction

Table 2.3 Data used for performance analysis.

| Nomenclature | Symbol | value |
|-----------------------------------|--------------|---------------------------------|
| Transmittance absorptance product | $\tau\alpha$ | 0.85 |
| Emissivity of absorber plate | ϵ_p | 0.95 |
| Solar radiation intensity | G | 1000 W/m ² |
| Density of air | ρ | 1.1788 / ³ |
| Thermal Conductivity of Air | k | 0.02624W/m-k |
| Dynamic Viscosity of Air | μ | 18.45 × 10 ⁻⁶ kg/m-s |
| Specific heat of air | C_p | 1.005 KJ/kg-k |
| Prandtl number | pr | 0.71 |
| Reynolds number | Re | 3000-12000 |
| Wind flow velocity | v_w | 2.17m/s |

3.1 Result and Discussion

Using obtained co-relations thermo-hydraulic performance viz. Average Nusselt number and average friction factor are calculated against Reynolds number for different relative roughness height and relative roughness. Temperature Enhancement Factor is plotted against Reynold's Number. Thermal Efficiency is also plotted against Reynold's Number. A comparison is also made between one side bend roughened duct with one side straight fin roughened duct having similar dimensions and with a smooth duct of same dimension.

3.1.1 Contours of Temperature and Pressure

Temperature Contour of Bend Roughened Duct

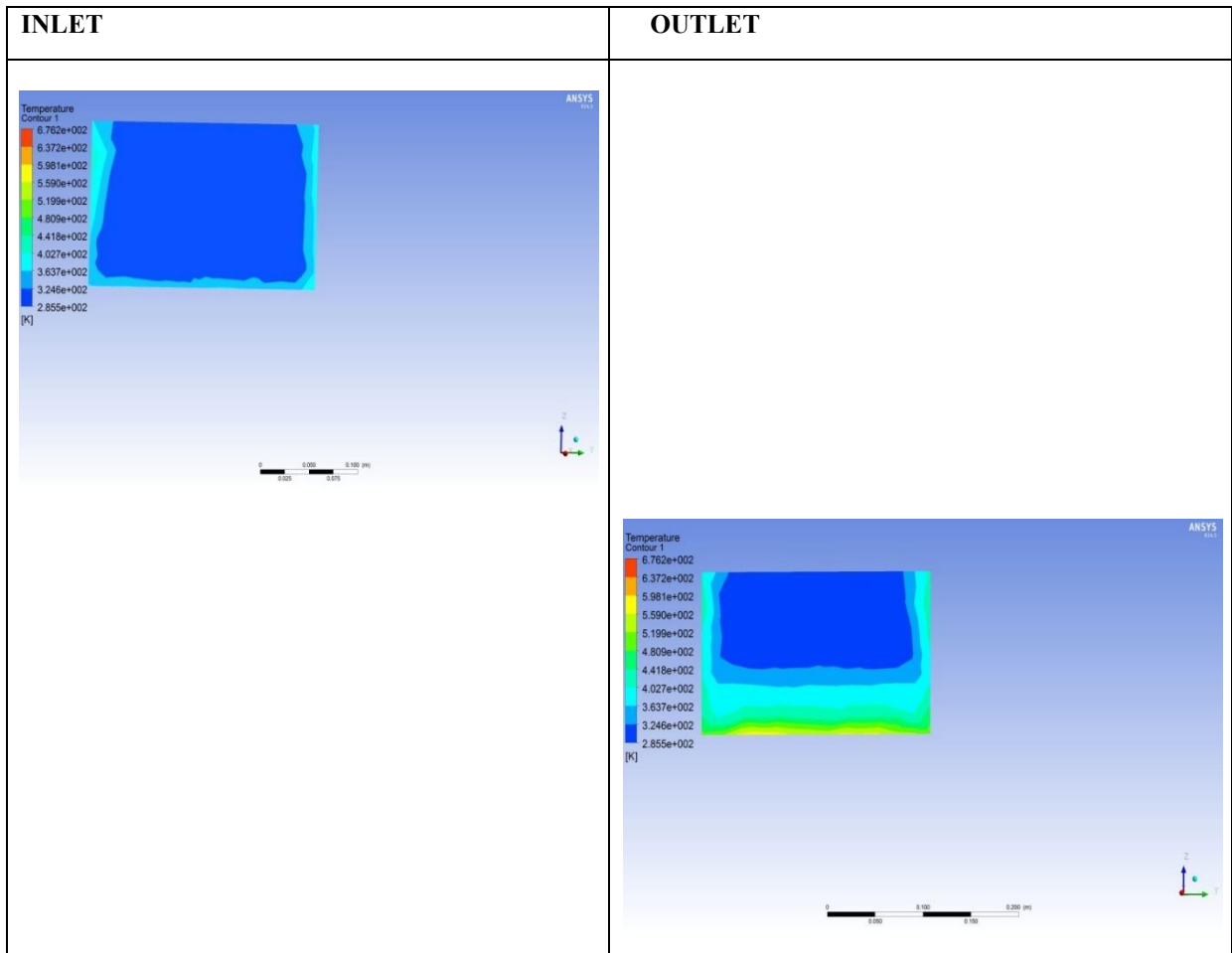


Figure 3.1 Temperature couter

Temperature Contour of Straight Fin Roughened Duct

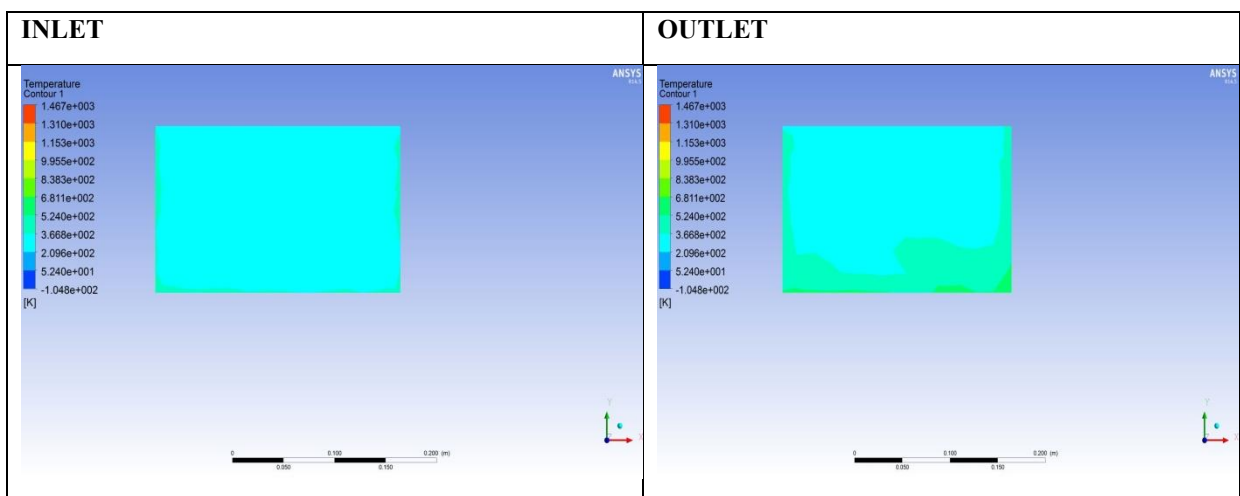


Figure 3.2 Temperature couter

Temperature Contour of Smooth Duct

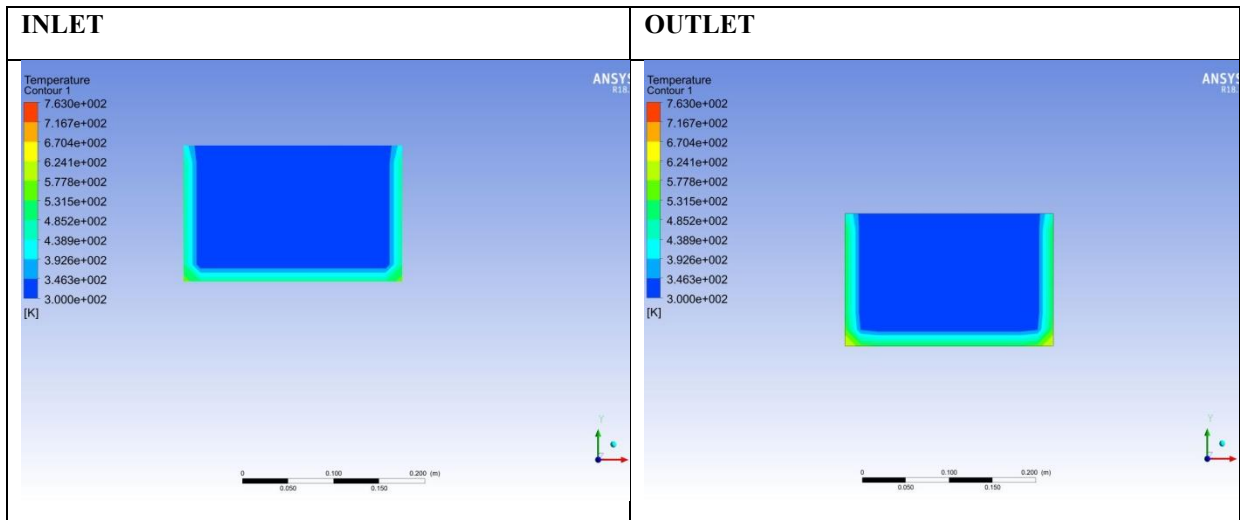


Figure 3.3 Temperature couture

Pressure Contour of Bend Roughened Duct

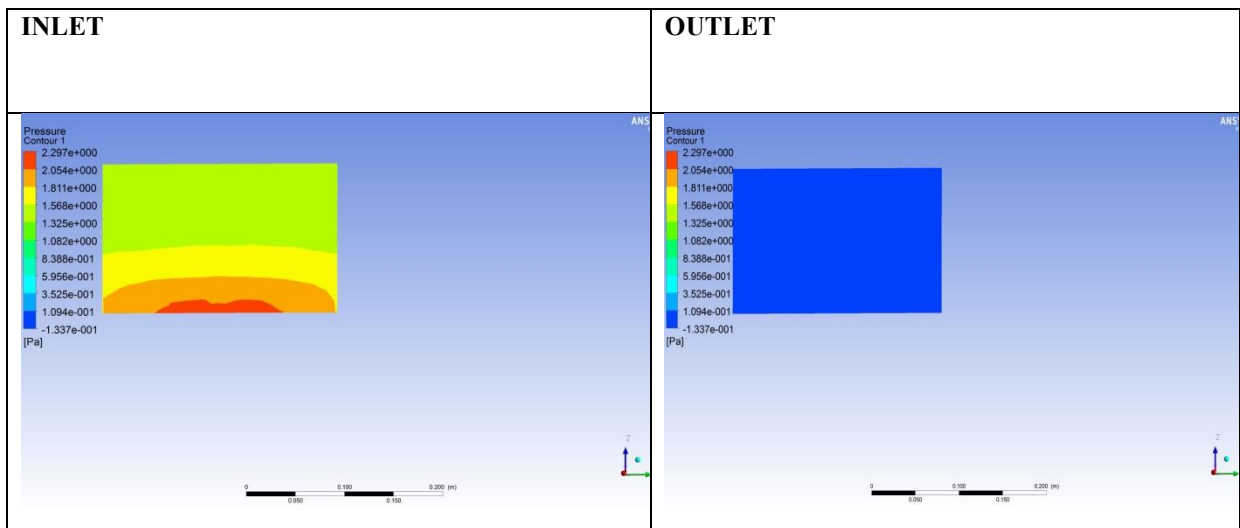


Figure 3.4 Pressure couture

Pressure Contour of Straight Fin Roughened Duct

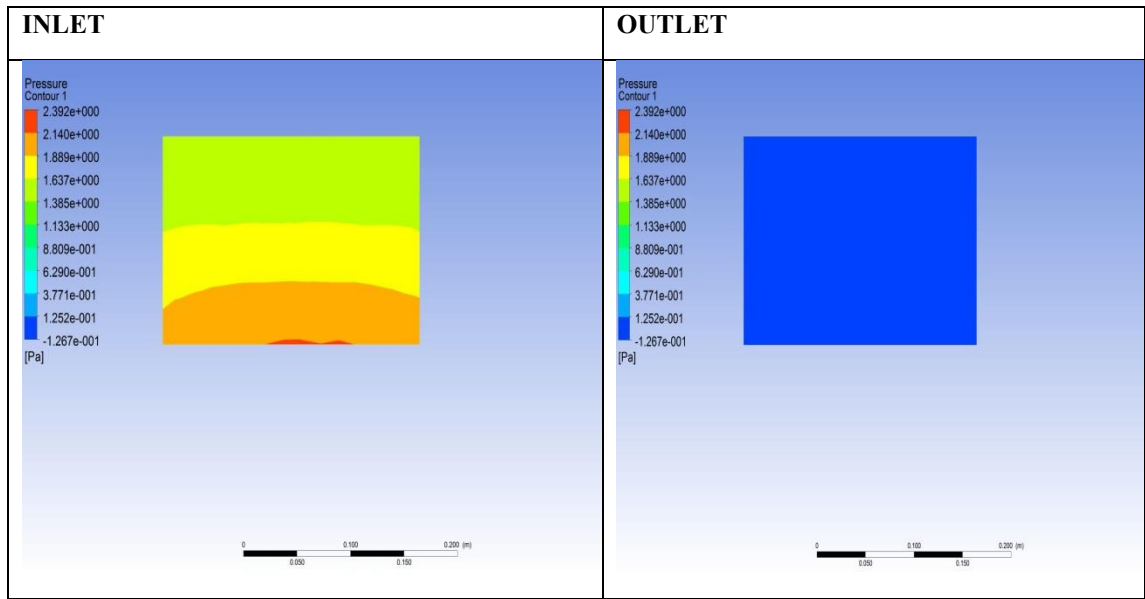


Figure 3.5 Pressure couter

Pressure Contour of Smooth Duct

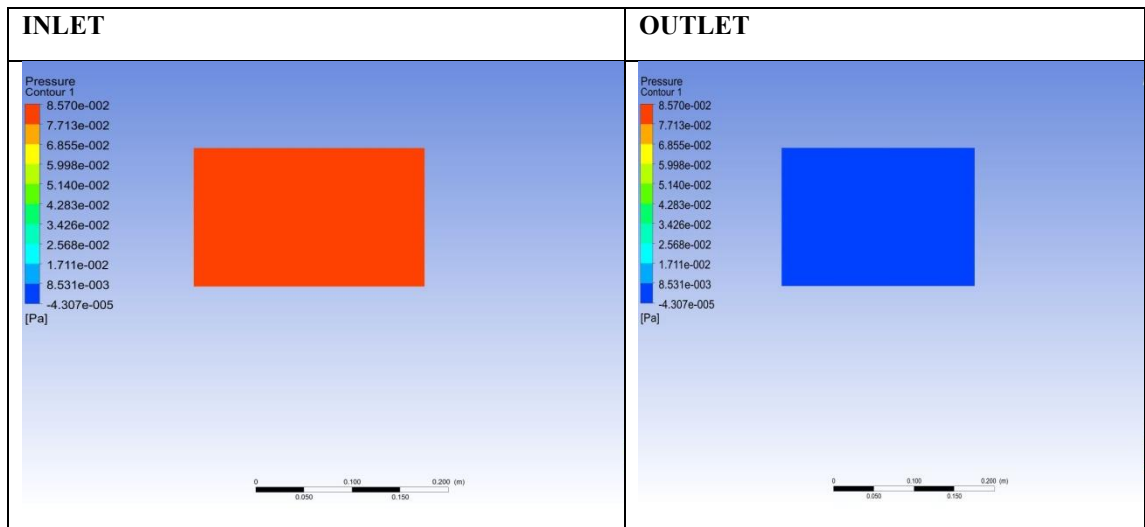


Figure 3.6 Pressure couter

Streamline

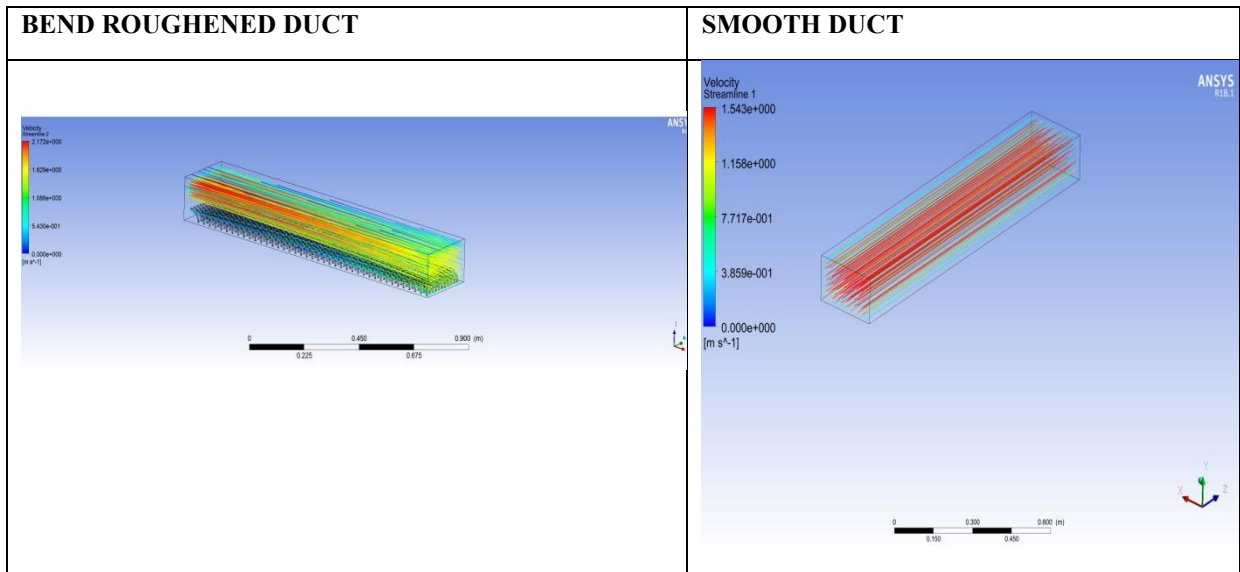


Figure 3.7 Streamline couter

3.1.2 Variation of Friction Factor with Reynold's Number for Different p/D_b

The graph shows that the friction factor decreases slightly with increasing Reynolds number for all cases, indicating turbulent flow behavior shown in figure 4.8.

However, the P/D ratio has a much stronger effect on friction factor than Reynolds number. As P/D

decreases ($12 \rightarrow 6 \rightarrow 4.29$), the friction factor increases significantly. The smooth pipe has the lowest friction factor, while $P/D = 4.29$ has the highest.

In conclusion, closer rib spacing (lower P/D) increases turbulence and wall resistance, leading to a higher friction factor, whereas smoother surfaces result in lower flow resistance.

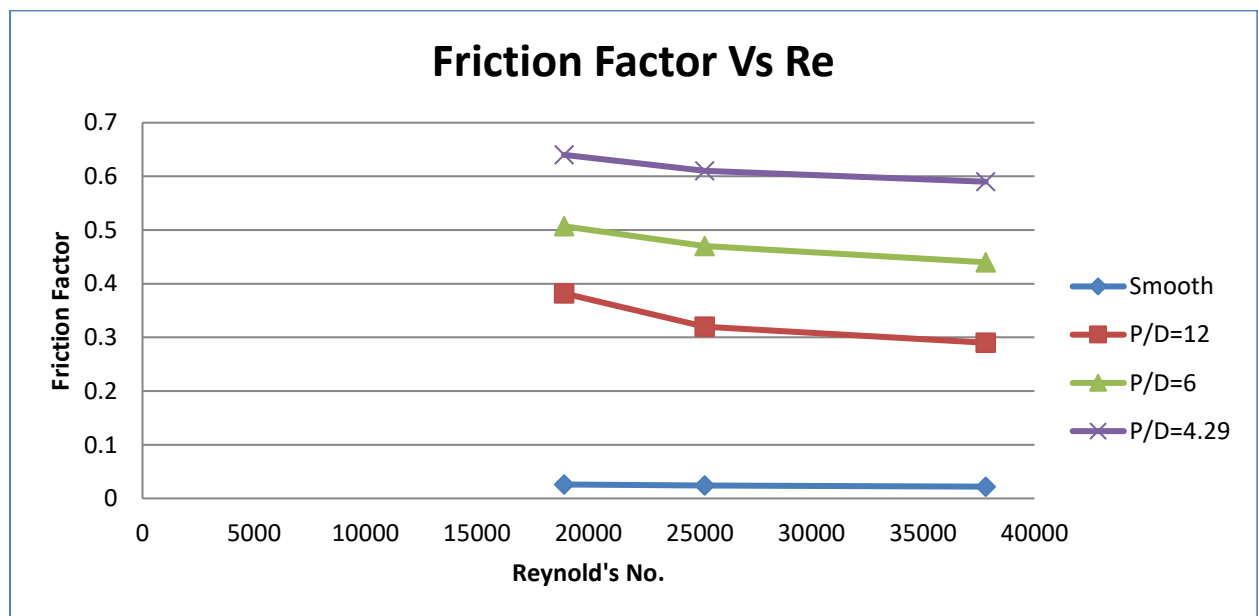


Figure 3.8 Friction Factor with Reynold's Number

3.1.3 Variation of Friction Factor with Reynold's Number for Different p/h

The graph shows that the friction factor decreases slightly as Reynolds number increases for all configurations, confirming turbulent flow behavior shown in figure 3.9

However, the P/h ratio strongly influences the friction factor:

- As P/h decreases (3 → 0.5), the friction factor increases significantly.

- P/h = 0.5 gives the highest friction factor.
- Smooth pipe shows the lowest friction factor.

This means that smaller P/h ratios (closer rib spacing relative to height) create more turbulence and higher flow resistance, leading to greater friction losses.

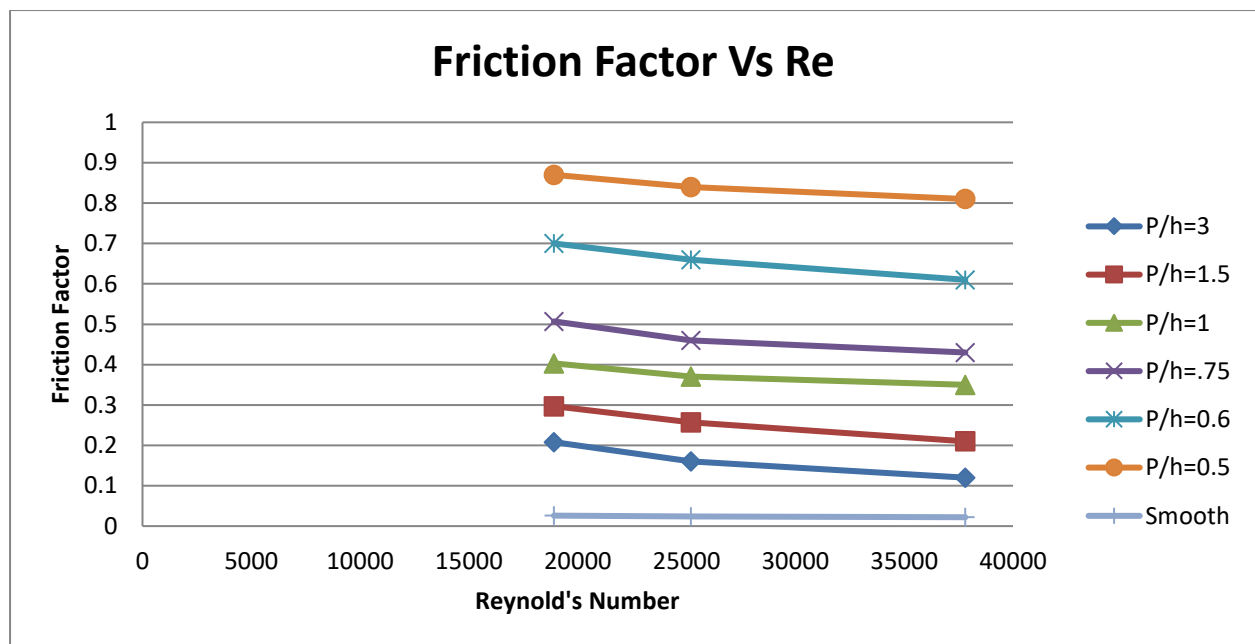


Figure 3.9 Friction Factor with Reynold's Number

3.1.4 Variation of Nusselt Number with Reynold's Number

The graph shows that the Nusselt number (Nu) increases with increasing Reynolds number (Re) for all methods, indicating improved heat transfer at higher flow rates shown in figure 3.10

Among the three approaches:

- Dittus–Boelter correlation predicts the highest Nusselt number.

- SST model gives slightly lower values than Dittus–Boelter.

- k-ε model predicts the lowest Nusselt number.

As Reynolds number increases, convective heat transfer improves. While all methods show the same increasing trend, the Dittus–Boelter correlation gives the highest heat transfer prediction, followed by SST, with k-ε providing the lowest estimates.

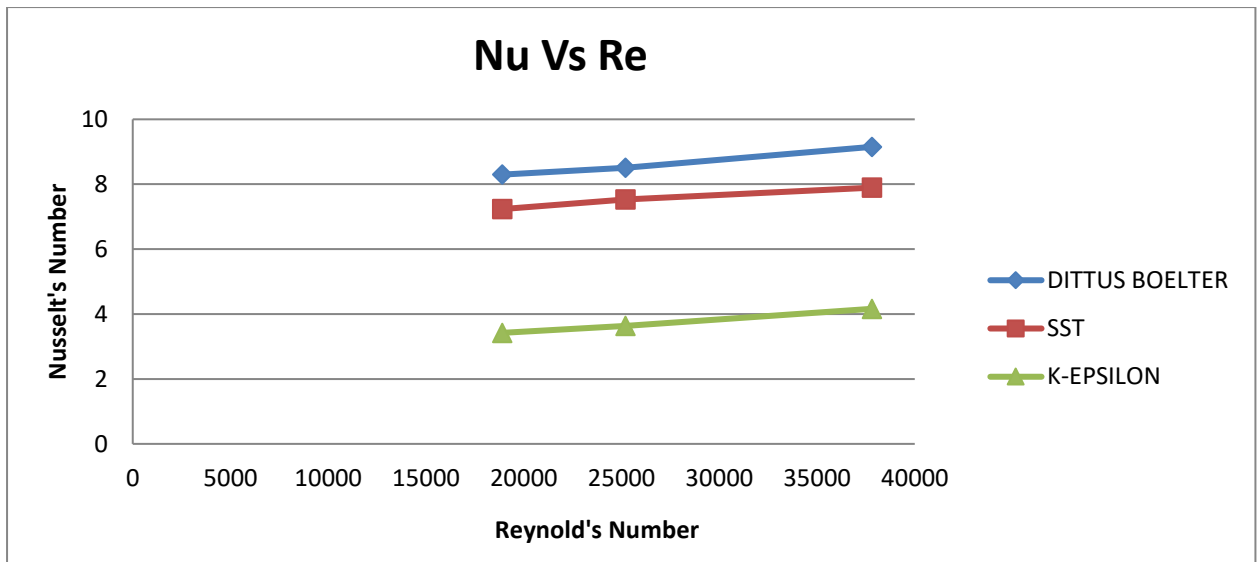


Figure 3.10 Nu with Reynold's Number

3.1.5 Variation of Temperature Enhancement Factor with Reynold's Number

The graph shows the variation of Temperature Enhancement Factor (TEF) with Reynolds Number (Re) for three surface conditions: Smooth Surface, Straight Roughened Surface and Bend Roughened Surface. TEF decreases with increasing Reynolds number for all three cases. Bend Roughened surface shows the highest temperature enhancement at all Reynolds numbers. Straight Roughened surface performs better than Smooth surface, but lower than Bend Roughened. Smooth

surface has the lowest enhancement factor throughout the range. The difference between roughened and smooth surfaces becomes slightly more noticeable at lower Reynolds numbers shown in figure 3.11

Surface roughening significantly improves heat transfer performance compared to a smooth surface. Among the three configurations, bend roughening provides the maximum temperature enhancement, making it the most effective design for improving thermal performance.

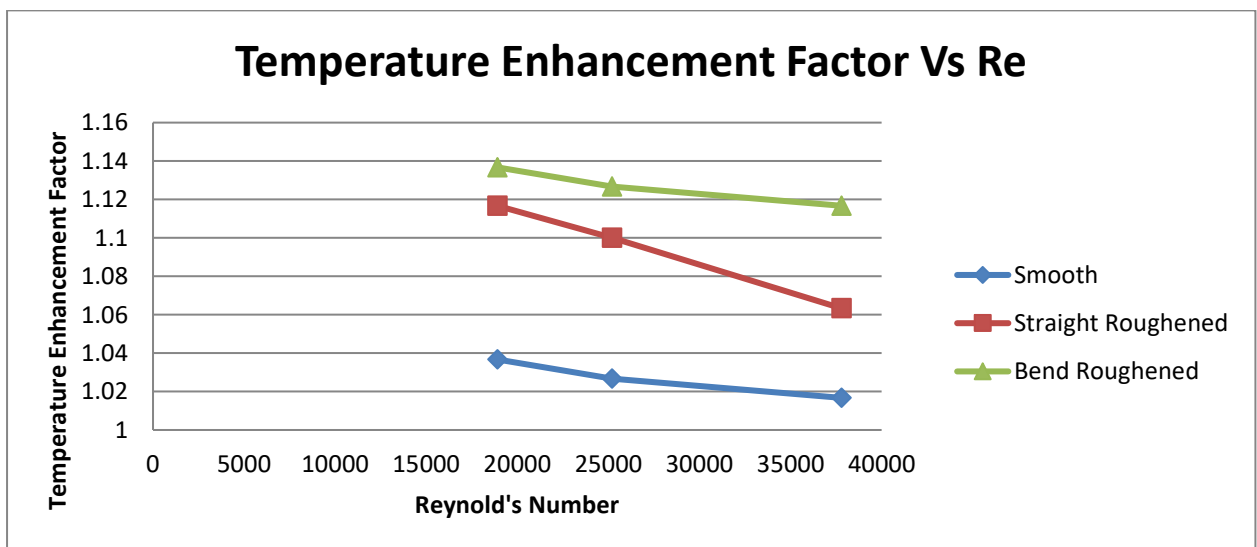


Figure 3.11 Temperature enhancement factor with Reynold's Number

3.1.6 Variation of Thermal Efficiency with Reynold's Number

The graph shows the relationship between Thermal Efficiency (%) and Reynolds Number (Re) for three configurations: Bend Roughened, Straight Fin Roughened, and Smooth surface shown in figure 3.12. Thermal efficiency increases with increasing Reynolds number for all configurations. Bend Roughened surface achieves the highest efficiency at all Reynolds numbers (approximately 38% to 41%). Straight Fin Roughened surface shows moderate performance, increasing from about 30%

to 36%. Smooth surface has the lowest efficiency, with only a slight increase (around 15% to 16%). The improvement in efficiency is significantly higher in roughened surfaces compared to the smooth surface.

Surface roughening enhances thermal performance considerably. Among the tested configurations, bend roughening provides the best thermal efficiency, making it the most effective design for improved heat transfer at higher Reynolds numbers.

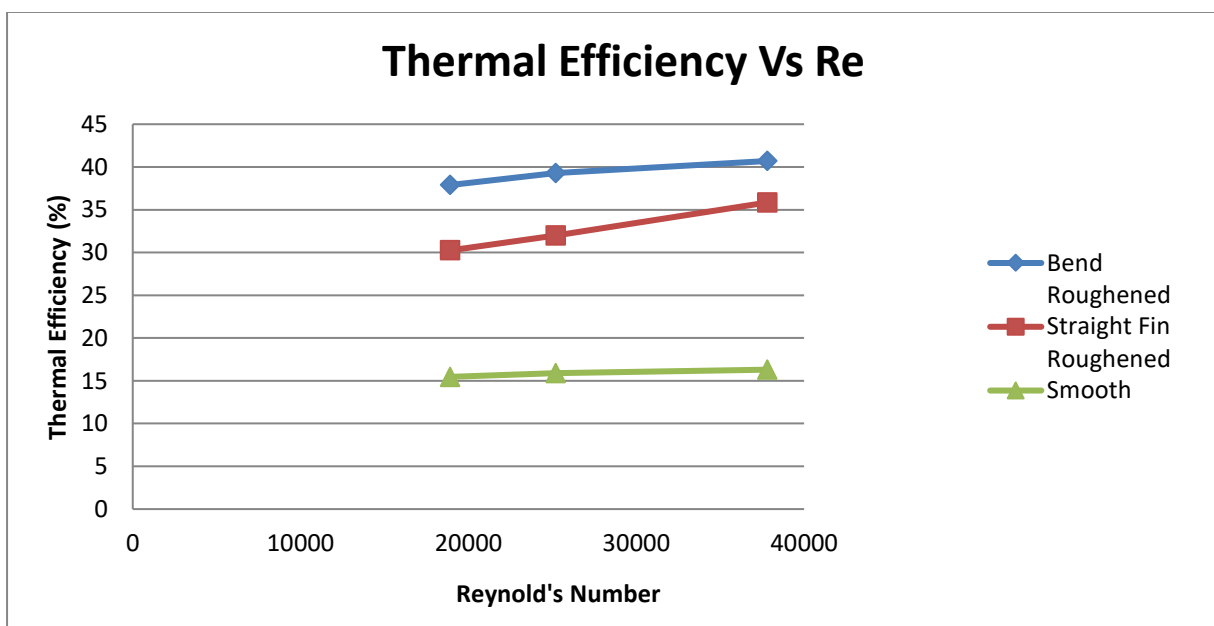


Figure 3.12 Thermal efficiency with Reynold's Number

4 Conclusions

On the basis of the results obtained the following conclusion has drawn

- Heat transfer and fluid flow analysis of rectangular solar air heater duct having one side artificially roughened surface has been done.
- The graph obtained plotting Friction Factor Vs Reynold's Number has consistency with a decreasing nature for different roughness parameter in case of different roughness element.
- A graph was plotted for Nusselt number Vs Reynold's Number for different viscous model

and was found to be increasing in nature for each case.

- There was an increasing variation of Temperature Enhancement Factor with Reynold's Number without any critical point or point of inflection.
- An increasing nature was found for the graph plotted for the variation of thermal efficiency with Reynold's Number.

Future scope of the project

In the present work performance analysis of solar air heater having bend roughness on one side of the duct is carried out. In future an attempt can be

made to optimize the parameters or characteristics present on the ordinates of the various graphs plotted.

5. References

- [1] Bopche SB, Tandale MS. Experimental investigations on heat transfer and frictional characteristics of turbulent roughened solar air heater duct. *Int J Heat Mass Transf* 2009;52:2834–48.
- [2] Twidell J, Weir T. Renewable energy sources. 2nd ed. New York: Taylor & Francis; 2006.
- [3] Sukhatme SP, Nayak JP. Solar Energy. 3rd ed. New Delhi: Tata McGraw Hill; 2011.
- [4] Duffie JA, Beckman WA. Solar engineering of thermal processes. 2nd ed. New York: Wiley; 1980.
- [5] Webb RL, Eckert ERG. Application of rough surface to heat exchanger design. *Int J Heat Mass Transf* 1992;15(9):1647–58.
- [6] Gawande VB, Dhoble AS, Zodpe DB. Effect of roughness geometries on heat transfer enhancement in solar thermal systems—a review. *Renew Sustain Energy Rev* 2014;32:347–78.
- [7] Ong KS. Thermal performance of solar air heaters: mathematical model and solution procedures. *Sol Energy* 1995;55(2):93–109
- [8] Bhushan B, Singh R. Thermal and thermo hydraulic performance of roughened solar air heater having protruded absorber plate. *Sol Energy* 2012;86:3388–96.
- [9] Ammari HD. A mathematical model of thermal performance of a solar air heater with slats. *Renew Energy* 2003;28:597–1615.
- [10] Shamardan MM, Norouzi M, Kayhani MH, Delouei AA. An exact analytical solution for convective heat transfer in rectangular ducts. *Zhejiang Univ-Sci A* 2012;13(10):768–81 (*ApplPhysEng*).
- [11] Patankar SV. Numerical heat transfer and fluid flow. Washington DC: Hemisphere; 1980.
- [12] Yadav AS, Bhagoria JL, CFD A. (computational fluid dynamics) based heat transfer and fluid flow analysis of a solar air heater provided with circular transverse wire rib roughness on the absorber plate. *Energy* 2013;55:1127–42
- [13] McAdams WH. Heat transmission. New York: McGraw-Hill; 1942.
- [14] Fox W, Pritchard P, McDonald A. Introduction to Fluid Mechanics. New York: John Wiley & Sons; 2010. p. 754.
- [15] ANSYS FLUENT 14.5. Documentation. Ansys, Inc; 2014.
- [16] ANSYS FLUENT 6.3, Solver setting, AnsysInc; 2006.
- [17] Yadav AS, Bhagoria JL. A numerical investigation of square sectioned transverse rib roughened solar air heater. *Int J ThermSci* 2014;79:111–31.
- [18] Yadav AS, Bhagoria JL. Numerical investigations of flow through an artificially roughened solar air heater. *Int J Ambient Energy* 2013.
- [19] Arulanandam SJ, Hollands KGT, Brundrett E. A CFD heat transfer analysis of the transpired solar collector under no-wind conditions. *Sol Energy* 1999;67(1–30):93–100.
- [20] Wang Chongjie, Guan Zhenzhong, Zhao Xueyi, Wang Delin. Numerical simulation study on transpired solar air collector. *Renewable Energy Resources and a Greener Future. Vol. VIII-3-4* 2006, ICEBO, Shenzhen, China; 2006.
- [21] Chaube A, Sahoo PK, Solanki SC. Analysis of heat transfer augmentation and flow characteristics due to rib roughness over absorber plate of a solar air heater. *Renew Energy* 2006;31(3):317–31.
- [22] Chaube A, Sahoo PK, Solanki SC. Effect of roughness shape on heat transfer and flow friction characteristics of solar air heater with roughened absorber plate. *WIT Trans Eng Sci* 2006;53:43–51.
- [23] Varol Y, Oztop HF. A comparative numerical study on natural convection in inclined wavy and flat-plate solar collectors. *Building and Environmental* 2008;43:1535–44.
- [24] Kumar S, Saini RP. CFD based performance analysis of a solar air heater duct provided with artificial roughness. *Renew Energy* 2009;34:1285–91.
- [25] Karmare SV, Tikekar AN. Analysis of fluid flow and heat transfer in a rib grit roughened surface solar air heater using CFD. *Sol Energy* 2010;84:409–17
- [26] Soi A, Singh R, Bhushan B. Effect of roughness element pitch on heat transfer and friction characteristics of artificially roughened solar air heater duct. *Int J AdvEngTechnol* 2010;1(3):339–46.
- [27] Rajput RS, Bhagoria JL, Giri AK, Kumar A. Study of heat transfer and friction characteristic of various artificial roughness in solar air heater duct by using computational fluid dynamics (CFD) software. In: Proceedings of international conference on advances in renewable energy; June 2010.